Molecular Therapy
Oncolytics
Original Article

DCLK1 Regulates Tumor Stemness and Cisplatin Resistance in Non-small Cell Lung Cancer via ABCD-Member-4

Janani Panneerselvam,[1] Priyanga Mohandoss,[2] Ravi Patel,[1] Hamza Gillan,[1] Michael Li,[1] Kirtana Kumar,[1] DangHuy Nguyen,[1] Nathaniel Weygant,[1] Dongfeng Qu,[1] Kamille Pitts,[1] Stanley Lightfoot,[1] Chinthalapally Rao,[1,3] Courtney Houchen,[1,3] Michael Bronze,[1] and Parthasarathy Chandrakesan[1]

[1]Department of Medicine, Stephenson Cancer Center, University of Oklahoma Health Sciences Center, Oklahoma City, OK 73104, USA; [2]Department of Biomedical Engineering, SRM University, Chennai, India; [3]Department of Veterans Affairs Medical Center, Oklahoma City, OK 73104, USA

Chemoresistance cells have features similar to cancer stem cells. Elimination of these cells is an effective therapeutic strategy to clinically combat chemoresistance non-small cell lung cancer (NSCLC). Here, we demonstrate that *Doublecortin-like kinase1* (*DCLK1*) is the key to developing chemoresistance and associated stemness in NSCLC. DCLK1 is highly expressed in human lung adenocarcinoma and strongly correlated with stemness. Silencing *DCLK1* inhibits NSCLC cell primary and secondary spheroid formation, which is the prerequisite feature of tumor stem cells. *DCLK1* inhibition reduced NSCLC cell migration/invasion *in vitro* and induced tumor growth inhibition *in vivo*. NSCLC cells responded differently to cisplatin treatment; indeed, the clonogenic ability of all NSCLC cells was reduced. We found that the cisplatin-resistant NSCLC cells gain the expression of DCLK1 compared with their parental control. However, *DCLK1* inhibition in cisplatin-resistance NSCLC cells reverses the tumor cell resistance to cisplatin and reduced tumor self-renewal ability. Specifically, we found that *DCLK1*-mediated cisplatin resistance in NSCLC is via an *ABC subfamily member 4* (*ABCD4*)-dependent mechanism. Our data demonstrate that increased expression of *DCLK1* is associated with chemoresistance and enhanced cancer stem cell-like features in NSCLC. Targeting *DCLK1* using gene knockdown/knockout strategies alone or in combination with cisplatin may represent a novel therapeutic strategy to treat NSCLC.

INTRODUCTION

Lung cancer is the deadliest cancer in both men and women.[1] About 85% of lung cancers are non-small cell lung cancer (NSCLC), and the 5-year survival rate for all stages of NSCLC is less than 16%.[2] The existing first-line treatment for the majority of NSCLC patients remains limited to cisplatin chemotherapy. Although the initial response of cisplatin as an anti-tumor agent in NSCLC treatment is favorable, often patients develop resistance and fail to respond to therapy.[3,4] Indeed, the gain of stemness properties have been associated with the acquisition of chemoresistance.[5,6] The expression of pluripotency transcription factors, including OCT4, NANOG, SOX2, and MYC, is responsible for tumor stemness properties in lung adenocarcinoma (LUAD).[7] Recent reports suggested that tumor cells with self-renewal ability are highly resistant to conventional therapies and many targeted therapies.[8–10] Furthermore, recent studies have demonstrated that ATP-binding cassette (ABC) efflux transporters that actively pump various anticancer drugs, including platinum compound, out of tumor cells are the primary reason for the gain of cisplatin resistance and NSCLC progression.[11,12] Chemo-resistance and tumor relapse have severe adverse impacts on NSCLC patient outcomes.[13,14]

Doublecortin-like kinase1 (DCLK1) is a tumor stem cell (TSC) marker in the intestine and pancreas.[15,16] Additionally, DCLK1 is a functional protein kinase involved in the regulation of tumorigenesis, tumor stemness, and epithelial-mesenchymal transition (EMT) in cancers, including colon, pancreas, liver, and renal cancers.[17–22] Recent reports suggest that there is a functional link between EMT, tumor stemness, and the development of therapy resistance. However, the role of DCLK1 in NSCLC tumorigenesis, self-renewal, and therapy resistance is not known. Multiple datasets collected from The Cancer Genome Atlas (TCGA) database reveal that DCLK1 expression is massively increased in LUAD compared with normal adjacent lung tissues, suggesting that DCLK1 may be a potential target for the regulation of NSCLC progression, self-renewal, and associated therapy resistance. Human DCLK1 consists of short and long isoforms, each with a shared kinase domain.[23] The potential tumorigenic function of DCLK1 isoforms in solid tumor cancers is not clear and remains largely unknown in NSCLC. In the present study, we used human NSCLC tissue microarray with adjacent control tissues and cisplatin-resistant A549 NSCLC (A549-CR), H460, and H1299 human NSCLC cell lines, and MRC9 human non-malignant lung cell lines were obtained from American Type Culture

Received 20 February 2020; accepted 22 May 2020;
https://doi.org/10.1016/j.omto.2020.05.012.

Correspondence: Parthasarathy Chandrakesan, MPhil, PhD, Department of Medicine, Stephenson Cancer Center, University of Oklahoma Health Sciences Center, Oklahoma City, OK 73104, USA.
E-mail: parthasarathy-chandrakesan@ouhsc.edu

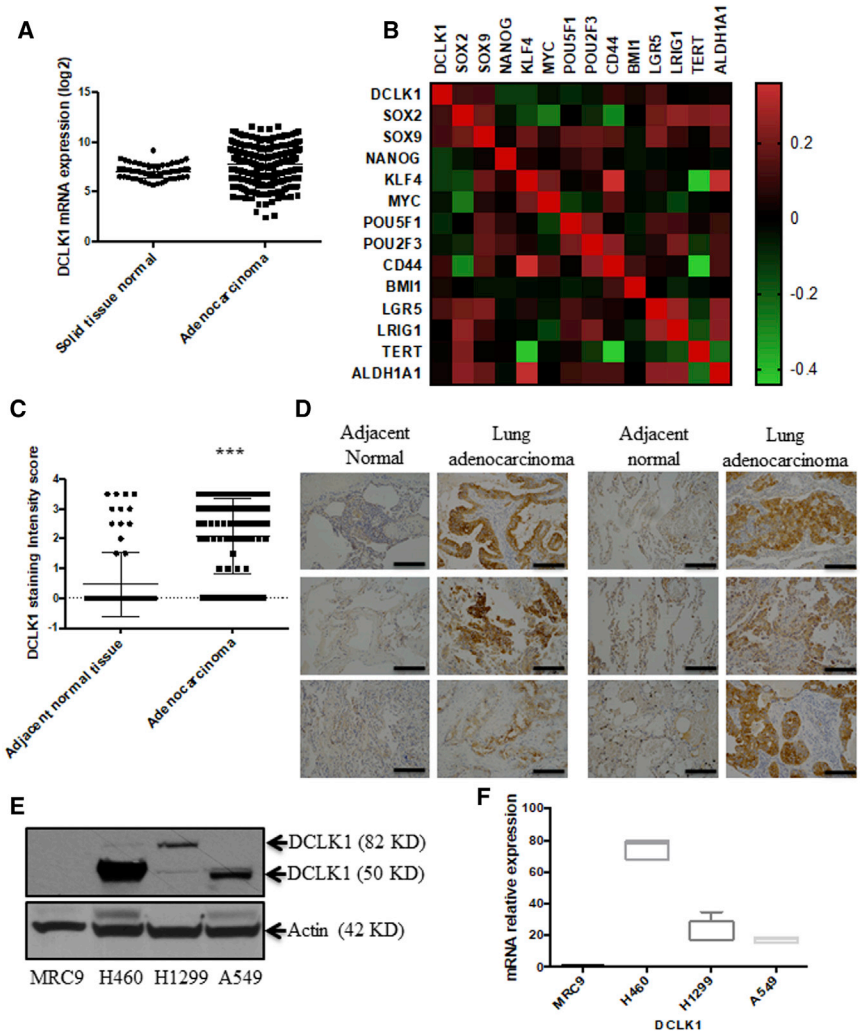

Figure 1. DCLK1 Expression Increased in NSCLC and Correlates with Stem Cell Factors

(A) DCLK1 mRNA expression is overexpressed in lung adenocarcinoma compared with adjacent solid lung normal tissue in the LUAD dataset collected from the TCGA database. (B) DCLK1 mRNA and mRNA of tumor stem cell markers (*CD44, BMI1, LGR5, LRIG1, TERT, ALDH1A1)* and pluripotency factors *(SOX2, SOX9, NANOG, KLF4, MYC, POU5F1, POU3F3*) were downloaded from the LUAD dataset of TCGA database. DCLK1 expression is positively correlated with genes of stem cell markers pluripotency factors. Color indicates a correlation of DCLK1 and other genes, negative (green) and positive (red). (C) Human tissue microarrays (TMAs) of lung adenocarcinoma and adjacent normal lung tissues were stained for DCLK1, and the intensity was scored. Immunohistochemistry reveals that DCLK1 is highly expressed ($p < 0.0001$) in lung adenocarcinoma compared with normal adjacent lung tissues. (D) Representative images of DCLK1 expression in normal and lung adenocarcinoma TMAs. Scale bars, 50 μm. (E) Expression of DCLK1 protein levels was assessed in a panel of NSCLC cell lines (H460, H1299, A549) and the non-malignant lung cell line MRC9 via immunoblot analysis. (F) Expression of DCLK1 mRNA levels assessed in a panel of NSCLC cell lines and the non-tumorigenic cell line. All quantitative data are expressed as mean ± SD of a minimum of five independent experiments. *$p < 0.05$,**$p < 0.01$, and ***$p < 0.001$ were considered statistically significant.

Collection (ATCC) and used for *in vitro* studies and *in vivo* xenografted studies. Here we demonstrate that DCLK1 is dysregulated in NSCLC, and specific inhibition of DCLK1 reduces self-renewal and cisplatin resistance. Given the importance of the gain of cisplatin resistance in NSCLC, this therapeutic strategy will have the potential to reverse the resistance to cisplatin by regulating the dysregulated DCLK1 and tumor stemness, critical players in therapy resistance and cancer high-grade progression.

RESULTS

DCLK1 Is Highly Expressed in Patients with LUAD

To understand the link between DCLK1 and LUAD, we analyzed DCLK1 mRNA expression in the human LUAD dataset from TCGA public database, which revealed that DCLK1 is highly expressed in LUAD compared with normal lung tissue (Figure 1A). TCGA database was utilized for the correlation analysis between DCLK1 and TSC markers/stemness factors in the LUAD dataset. Our analysis revealed that DCLK1 is strongly correlated with TSC markers *LGR5* and *CD44*, and tumor stemness factors *SOX9* and *SOX2* (Figure 1B). DCLK1 correlation was further strengthened by GeneMANIA network analysis in humans, which revealed that DCLK1 either directly (genetic and physical) or indirectly (via downstream targets) interacts with TSC markers and stemness factor (Figure S1A). We performed immunohistochemistry (IHC) for DCLK1 staining in the human LUAD tissues (n = 75 biopsies) and the normal adjacent tissues. We observed increased DCLK1 immunostaining ($p < 0.0001$) in human LUAD compared with normal adjacent tissues (Figures 1C and 1D). Increased expression of DCLK1 protein and mRNA was observed in NSCLC cell lines (H460, A549, and H1299) compared with the non-malignant lung cell line (MRC9) (Figures 1E and 1F). Interestingly, H460 and A549 cells demonstrated an increased expression of DCLK1 protein short-form (50 kDa), which is predominantly overexpressed in solid tumor cancers[19,24] compared with H1299 cells expressing the long-form (82 kDa). Protein expression analysis of DCLK1 short-form and long-form represents that H1299 cells express long-form and H460/A549 cells express short-form. However, the difference in the expression of DCLK1 isoform variance between the cell lines is not currently been investigated utilizing isoform-specific primers for mRNA expression analysis. Indeed, in most cancer-related studies, it is crucial to correlate mRNA expression with their respective protein expression due to post-translational modification

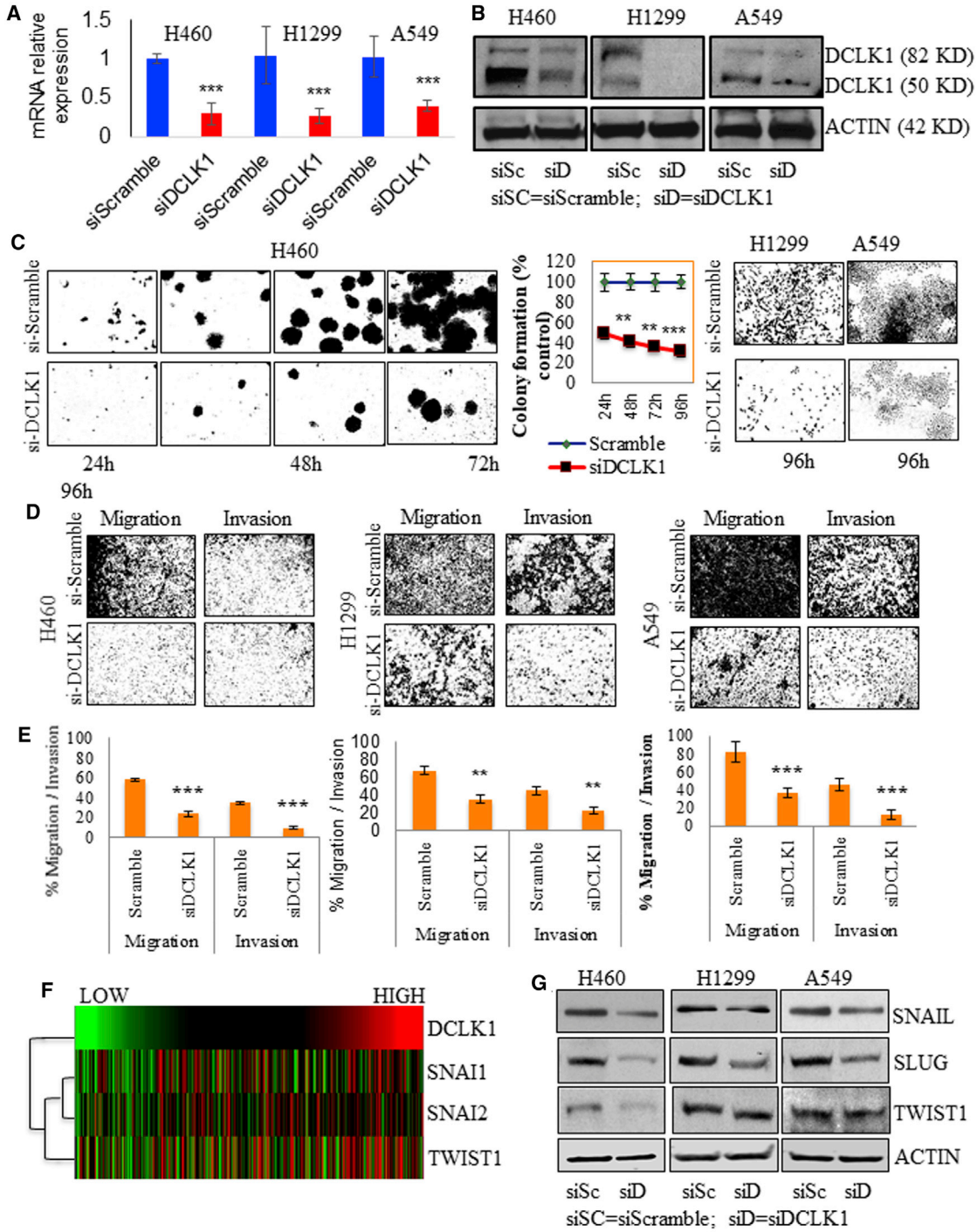

Figure 2. Specific Silencing of *DCLK1* Reduces NSCLC Migration, Invasion, and Colony Formation by Regulating EMT-Associated Factors

(A) Specific silencing of *DCLK1* in NSCLC cells reduced the mRNA expression of *DCLK1*. (B) DCLK1 inhibition reduced the protein expression in all three NSCLC cells. (C) siDLKC1 transfection in NSCLC cells reduced the colony formation in all three NSCLC cells. Line graph representing the percentage of colony formation for H460 cells. (D) siDLKC1 transfection in NSCLC cells reduced the tumor cell migration and invasion ability. (E) Bar graph representing the percentage of cell migration and invasion of NSCLC cells. (F) Heatmap of EMT factors mRNA expression levels by dividing lung cancer patients into two groups based on *DCLK1* expression levels from TCGA.

(legend continued on next page)

(PTM), stability, and ubiquitination. However, further molecular studies are required to know the DCLK1-associated PTM and its stability in lung cancer.

DCLK1 Regulates NSCLC Cell Proliferation, Migration, and Invasion

To investigate DCLK1's role in NSCLC proliferation, migration, and invasion, we utilized small interfering RNA (siRNA) against *DCLK1* (siDCLK1) in NSCLC cells. siDCLK1 treatment reduced the *DCLK1* mRNA and protein expression (Figures 2A and 2B) and cell proliferation by 40%–50% and colony-forming ability, which represents the cells' viability and survival, by 60%–80% compared with siRNA Scramble (siSCR)-transfected cells (Figure S1B; Figure 2C), but no changes were observed in MRC9 cells (Figure S2). DCLK1 knockdown significantly decreased (50%–60%) the migration and invasion of NSCLC cells compared with siSCR controls (Figures 2D and 2E). We found a strong correlation between *DCLK1* expression and EMT transcriptional factors *SNAI1, SNAI2,* and *TWIST* in the LUAD dataset from the TCGA database (Figure 2F). Furthermore, we observed that siDCLK1 treatment significantly reduced the expression of SNAI1 and SNAI2 in all NSCLC cells (Figure 2G). However, only H460 cells showed a significant reduction in TWIST expression following DCLK1 knockdown (Figure 2G).

Role of DCLK1 in Regulating Tumor Stemness

Self-renewal (clonogenicity) is a hallmark of stem cells, which can be measured by 3D spheroid culture.[25,26] Among the three cell lines, H460 cells showed more spheroid formation than A549 and H1299 cells *in vitro* under scramble RNA transfection (Figure S3A). Overall, DCLK1 knockdown in all three NSCLC cell lines reduced 80%–90% of their spheroid formation ability (Figures 3A, 3B, 3D, 3E, 3G, and 3H). The effect of DCLK1 knockdown-mediated reduction of spheroid formation ability is higher in H1299 compared with H460 and A549 cells. Furthermore, the number of clonal cells per spheroid was reduced in all three NSCLC cell lines after DCLK1 knockdown (Figures 3C, 3F, and 3I). Given the importance of DCLK1 in the regulation of tumor stemness,[22,27] we evaluated the effect of DCLK1 knockdown on the stem cell markers and pluripotency factors in NSCLC cells. DCLK1 knockdown in NSCLC cells reduced the expression of stem cell markers LGR5, CD44, and BMI1 and pluripotency factors SOX2, NANOG, and OCT4 compared with siSCR controls (Figures 3J and 3K).

DCLK1 Knockdown Inhibited the TSC Phenotype and Reduced the Size of NSCLC Tumor Xenograft

Tumor cells with the TSC phenotype have the ability to form secondary tumorspheres.[28,29] To investigate the role of DCLK1 in NSCLC secondary spheroid formation, we knocked down DCLK1 in NSCLC primary spheroids derived from A549 and H460 cells. DCLK1 knockdown in the primary spheroids completely abrogated secondary spheroid formation (Figures 4A and 4C). We observed that the primary spheroid cells have 2- to 3-fold secondary spheroid-forming ability compared with primary cells to form primary spheroids (Figures 4B and 4D). Interestingly, we observed a 9- to 14-fold increase in the expression of DCLK1 mRNA in the primary and the secondary spheroids compared with parental NSCLC cells (Figures S3B and S3C). To assess the importance of DCLK1 in the NSCLC tumorigenesis *in vivo*, we conducted a tumor xenograft study. We intraperitoneally (i.p.) injected the tumor-bearing mice with siDCLK1-poly(lactide-co-glycolide acid) (PLGA) nanoparticles (siD-NPs), which resulted in tumor regression compared with siSCR-PLGA NPs (siSCR-NPs) treatment (Figures 4E and 4F).

DCLK1 Is Required for the Development of Resistance to Cisplatin in NSCLC Cells

Cisplatin is the most commonly used treatment regimen for lung cancer.[30] However, there are several reports contrary to the effect of cisplatin on the viability of cancer cells between two-dimensional (2D) and three-dimensional (3D) cultures.[31,32] Indeed, 3D cell culture could relate better to *in vivo* models than 2D cell cultures.[33] Therefore, we first want to investigate the differential anti-cancer effect of cisplatin between 2D and 3D cell cultures of NSCLC cell lines. Cisplatin treatment significantly reduced the colony-forming ability of NSCLC cells in the 2D culture system even at the lower concentration of 1 μM treatment and reduced further with 5 μM treatment (Figures S4A and S4B). H1299 cells are the most sensitive even at 1 μM cisplatin. At a 10-μM concentration of cisplatin treatment, all NSCLC cells significantly suffered to form a colony in the 2D culture system (Figures S4A and S4B). The clonogenic ability of the H1299 cells in 3D culture system was significantly reduced at 1- and 5-μM cisplatin concentrations (Figures S4C and S4D). At a 10-μM concentration of cisplatin treatment, H1299 cells are able to maintain only 12% of their clonogenic ability compared with vehicle treatment (Figures S4C and S4D). However, H460 and A549 NSCLC cells responded with better resistance to cisplatin and can maintain their clonogenic ability between 34% and 40% even at a 10-μM concentration of cisplatin treatment (Figures S4C and S4D). Although the response to cisplatin treatment between the NSCLC cells differs, the variations to cisplatin tolerance could be better understood by a 3D culture system than the 2D system.

Next, we investigated the role of DCLK1 in the development of NSCLC cisplatin resistance. We generated A549-CR, generated a dose-response curve, and calculated half maximal inhibitory concentration (IC_{50}) concentrations (Figures 5A and 5B). A549-CR cells exhibited a 9-fold higher IC_{50} concentration (57.42 μM) for cisplatin than that of parental A549 cells (6.086 μM) (Figure 5A). Cisplatin resistance in A549-CR cells enhanced fibroblastoid-like

DCLK1 mRNA expression is positively correlated with genes of epithelial-mesenchymal transition transcriptional factors *SNAI1, SNAI2,* and *TWIST*. (G) DCLK1 inhibition reduced the protein expression levels of SNAIL and SLUG in all three NSCLC cells. However, DCLK1 inhibition reduced the expression of TWIST in only H460 cells. All quantitative data are expressed as mean ± SD of a minimum of five independent experiments. *$p < 0.05$, **$p < 0.01$, and ***$p < 0.001$ were considered statistically significant.

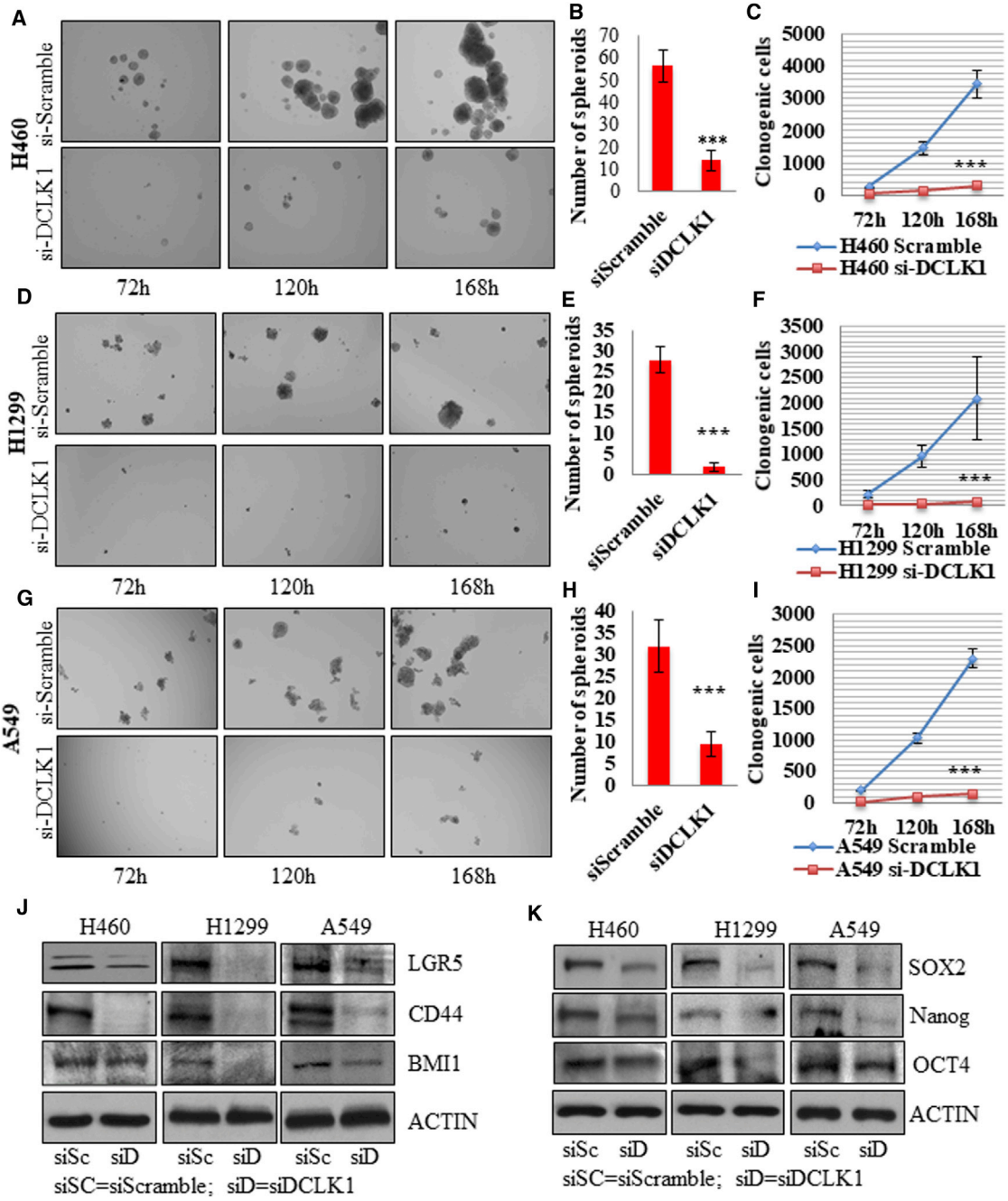

Figure 3. DCLK1 Inhibition Reduces NSCLC Cell Self-Renewal and the Expression of Stem Cell Markers and Pluripotency Factors

(A) Specific inhibition of DCLK1 reduced the self-renewal of H460 cells. (B) Bar graph representing the number of spheroids between siSCR- and siDCLK1-treated H460 cells. (C) Line graph representing the number of clonogenic cells between siSCR- and siDCLK1-treated H460 cells. (D) Specific inhibition of DCLK1 reduced the self-renewal of H1299 cells. (E) Bar graph representing the number of spheroids between siSCR- and siDCLK1-treated H1299 cells. (F) Line graph representing the number of clonogenic cells between siSCR- and siDCLK1-treated H1299 cells. (G) Specific inhibition of DCLK1 reduced the self-renewal of A549 cells. (H) Bar graph representing the number of spheroids between siSCR- and siDCLK1-treated A549 cells. (I) Line graph representing the number of clonogenic cells between siSCR- and siDCLK1-treated A549 cells. (J) DCLK1 inhibition significantly reduced the protein expression levels of tumor stem cell markers LGR5 and CD44 in all three NSCLC cells. Expression levels of BMI1 show a moderate reduction in H460 cells but are significantly reduced in H1299 and A549 following siDCLK1 transfection. (K) DCLK1 inhibition significantly reduced the protein expression levels of pluripotency factors SOX2, NANOG, and OCT4 in all three NSCLC cells. All quantitative data are expressed as mean ± SD of a minimum of five independent experiments. *$p < 0.05$, **$p < 0.01$, and ***$p < 0.001$ were considered statistically significant.

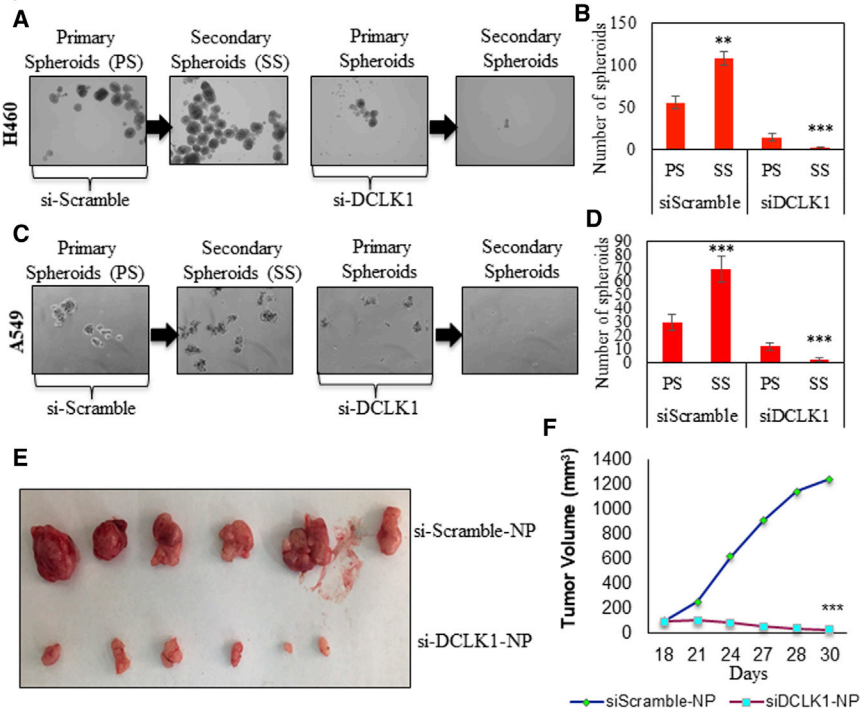

Figure 4. Silencing DCLK1 Inhibits NSCLC Cell Secondary Spheroid Formation *In Vitro* and Tumor Growth *In Vivo*

Tumor stem cells are capable of generating next-generation spheroids called secondary spheroids. (A) Specific inhibition of DCLK1 reduced the number of H460 NSCLC tumor cell primary spheroids and completely abrogated the secondary spheroid formation. (B) Bar graph representing the number of primary and secondary spheroids between siSCR- and siDCLK1-treated H460 cells. (C) Specific inhibition of DCLK1 reduced the number of A549 NSCLC tumor cell primary spheroids and completely abrogated the secondary spheroid formation. (D) Bar graph representing the number of primary and secondary spheroids between siSCR- and siDCLK1-treated A549 cells. (E) H460 cells were subcutaneously injected into athymic nude mice (number of mice = 10) and allowed to grow until the tumor reached an average volume of 100 mm^3. siDCLK1-NP treatment of the H460 tumor xenografts significantly regressed tumor growth. (F) Line graph representing the reduced tumor volume of siDCLK1-NP-treated xenograft mice compared with siSCR-NP-treated xenograft mice. All quantitative data are expressed as mean ± SD of a minimum of three independent experiments. *$p < 0.05$, **$p < 0.01$, and ***$p < 0.001$ were considered statistically significant.

morphology and reduced proliferation (Figures 5B and 5C; Figure S5). Furthermore, the difference in whole-cell cisplatin accumulation between A549-CR and its parental counterpart was quantified using Cisplatin Assay Kit (ProFoldin USA). After 24-h cisplatin treatment, we observed a significant reduction in the uptake of cisplatin by A549-CR cells when compared with A549 parental cells (Figure S6A). Further, A549-CR cells showed a 3- to 4-fold increase in clonogenic ability compared with parental cells (Figure 5D). Thus, the change in morphology and slow cycling of A549-CR cells is closely associated with the stem-like signature of enhanced self-renewal capacity. Interestingly, we observed a significant increase in protein and mRNA expression of *DCLK1* in the A549-CR cells compared with parental cells. This is the first report to show the DCLK1 higher expression in the CR NSCLC cells (Figure 5E), suggesting that *DCLK1* expression is the key factor involved in the gain of cisplatin resistance. Furthermore, knockdown of *DCLK1* in A549-CR cells resulted in a ~20% reduction in cell viability, whereas cisplatin (40 μM) alone treatment resulted in a ~16% reduction (Figure 5F). A combination of siDCLK1 + low-dose cisplatin treatment (5 μM, which is an 11-fold reduced dose than the original IC_{50} concentration of 57.42 μM) resulted in a ~86% decrease in cell viability compared with vehicle control (Figure 5F). However, the combination treatment of siDCLK1 + low-dose cisplatin (5 μM) resulted in a ~6% decrease in MRC9 cell viability (Figure S6B), suggesting that the combinatorial therapeutic agents are more specifically targeting the tumor cells than the normal cells. We observed that a combination of siDCLK1 + low-dose cisplatin (5 μM) treatment abrogated the CR NSCLC cell self-renewal by 95% compared with siDCLK1 alone (71%) and cisplatin (40 μM) alone (41.4%) (Figures 5G and 5H).

DCLK1 Induces Cisplatin Resistance in NSCLC Cells via the ABCD4-Dependent Mechanism

Previous studies have shown the role of ABC transporters in the development of resistance to cisplatin in various solid tumor cancers, including lung cancer.[11,12,34] ABC transporters are one of the largest families of membrane-bound proteins in humans that catalyze the ATP-dependent transport of a wide variety of substrates.[35] Recently, several members of the ABC transporters have been found to contribute to governing the movement of platinum drugs and their metabolites across biological membranes to limit its cytotoxic efficacy and adverse drug reactions in cancer cells.[35,36] Because we demonstrated that DCLK1 knockdown in A549-CR cells showed an increased sensitivity to cisplatin and reduced cell viability and self-renewal, next we wanted to investigate the role of DCLK1 on the regulation of ABC transporters in the gain of NSCLC cisplatin resistance, which remains unknown. Therefore, we analyzed the TCGA LUAD RNA sequencing (RNA-seq) dataset for Pearson r correlation (Figure 6A; Figure S6C). We observed that *DCLK1* is strongly correlated with *ABCA1, ABCA12, ACBA6, ABCB6, ABCC11, ABCC5*, ABC subfamily member 4 (*ABCD4*), *ABCF2, ABCG4, and ABCG8* in the LUAD dataset. To further investigate the connection between *DCLK1* and the ABC transporters, we used the GeneMANIA webserver to predict interactions between *DCLK1* and ABC transporters in the network using the parameters limited to physical interactions, co-expression, shared protein domain, and pathways to score nodes

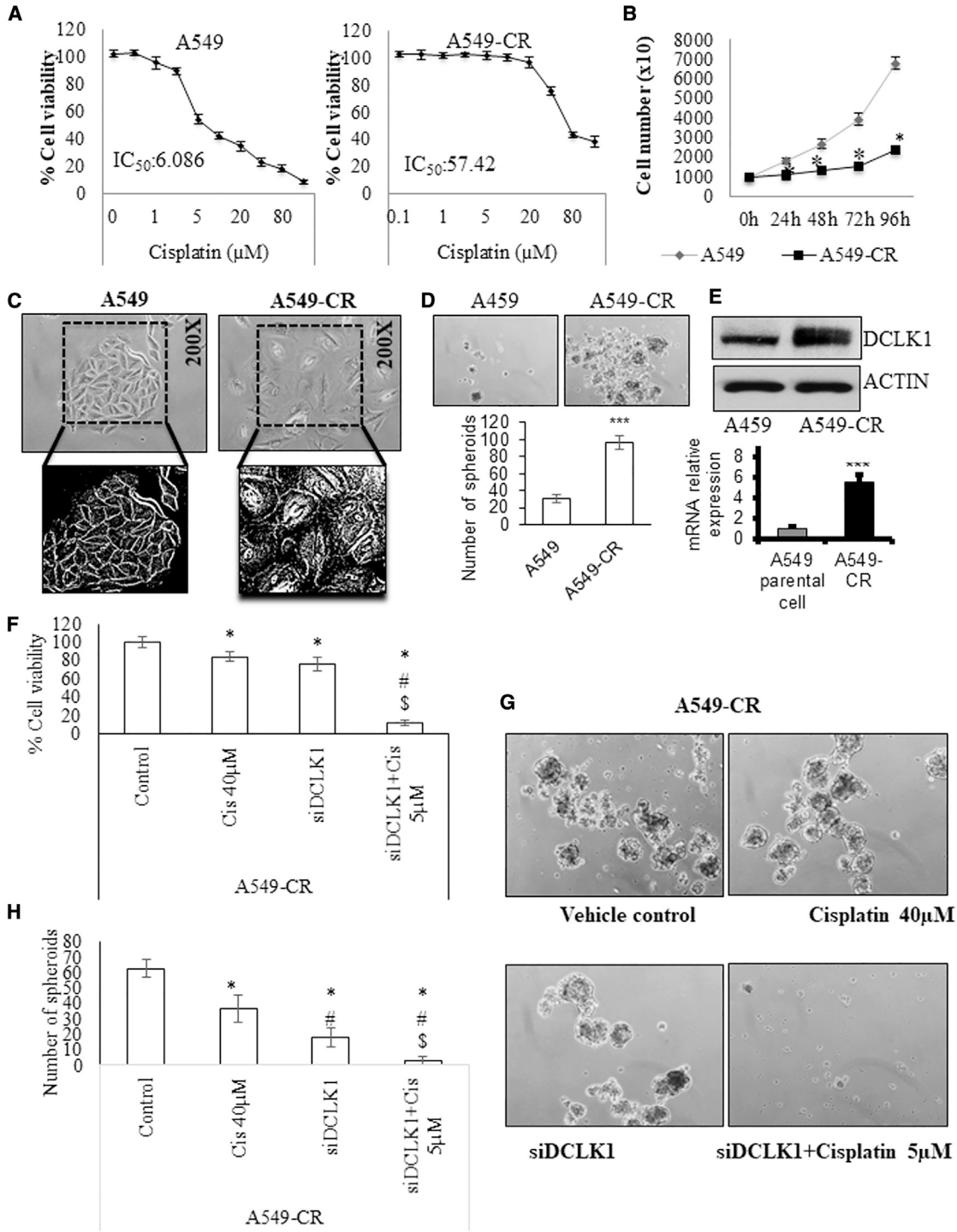

Figure 5. DCLK1 Regulates the Gain of Cisplatin Resistance, and DCLK1 Targeting in A549-CR Cells Increased the Sensitivity to Cisplatin Treatment

(A) Parental NSCLC (A549) cells and cisplatin-resistant A549 NSCLC (A549-CR) cells were treated with an increasing concentration of cisplatin (0.2–100 μM). Cell death was measured using the live/dead assay. Dose-response curves were generated from which IC_{50} values were deduced. (B) A549 and A549-CR cells were plated at equal numbers, and cell numbers were counted at different time intervals. Cisplatin resistance cells (A549-CR) display poor cell proliferation. (C) Cisplatin resistance NSCLC tumor cells (A549-CR) exhibited different morphology compared with the parental NSCLC tumor cells (A549); for more visibility, pictures were transformed into black and white pictures and cropped and enlarged. (D) A549-CR cells acquire enhanced tumor stem cell-like self-renewal features compared with parental A549 cells. Bar graph represents

(legend continued on next page)

and source organism *Homo sapiens* as additional parameters (Figure 6B). From the GeneMANIA network, we found that *DCLK1* has networked with ABC transporters, and *DCLK1* shows its interaction with ABC transporters via downstream factors/adaptor factors. Next, we profiled the protein expression levels of ABC transporters in the A549 parental cells, A549-CR cells, and A549-CR cells with and without DCLK1 knockdown (Figure 6C). As shown in Figure 6C, we found an increased expression of 10 ABC transporters (*ABCA1, ABCA12, ABCA8, ABCB6, ABCC11, ABCC5, ABCD4, ABCF2, ABCG4, and ABCG8*) and decreased expression of 6 ABC transporters (*ABCA2, ABCD3, ABCG2, ABCG5, CFTR, and TAP2*) in the A549-CR cells compared with A549 parental cells. Among them, the expression levels of *ABCD4* and *ABCG8* are highly increased in A549-CR cells compared with A549 parental cells. Interestingly, DCLK1 knockdown in A549-CR cells reversed the expression of increased ABC transporters. Note that the only ABC transporter, *ABCD4*, expression is strongly regulated by DCLK1 in the NSCLC cells (Figure 6C). Our protein expression analysis from the A549 parental cells, A549-CR cells, and A549-CR cells with DCLK1 knockdown further revealed that the expression of ABCD4 strongly depends on the DCLK1 expression levels in the NSCLC cells (Figure 6D). However, DCLK1 expression is not regulated by ABCD4 in the NSCLC cells, because ABCD4 knockdown in the A549-CR cells did not alter the expression levels of DCLK1 (Figure 6E). These data suggest that DCLK1 is not the downstream target to ABCD4; instead, DCLK1 silencing downregulates ABCD4 in CR cells. To understand whether DCLK1 mediates its therapy-resistant effects through ABCD4, we knocked down ABCD4 in the A549-CR cells, which resulted in ~10% reduction in cell viability compared with cisplatin (40 μM) alone treatment, which resulted in ~18% reduction in cell viability (Figure 6F). However, combination therapy using siRNA targeting human *ABCD4* (siABCD4) + low-dose cisplatin (5 μM) resulted in a ~78% decrease in cell viability (Figure 6F). Similarly, the combination treatment of siABCD4 + cisplatin (5 μM) reduced the self-renewal of CR NSCLC cells by ~72% compared with cisplatin alone by 41% and siABCD4 alone by 32% (Figures 6G and 6H). Taken together, these data suggest that DCLK1 mediated NSCLC cell cisplatin resistance, and associated enhanced self-renewal occurs via an ABCD4-dependent mechanism.

DISCUSSION

The development of drug resistance during chemotherapy against lung cancer is a major reason for the mortality associated with this disease.[37,38] The gain of cellular self-renewal properties has been associated with the acquisition of chemoresistance.[5,6,39] DCLK1 is a marker of TSCs in pancreas, and colon cancer plays a critical role in the self-renewal capacity of cells derived from these tumors.[15,16] In this study, we demonstrate that DCLK1 expression is increased in NSCLC patients and is associated with increased expression of TSC-related genes. Moreover, we provide evidence that the development of cisplatin resistance in NSCLC cells is marked by a distinct increase in DCLK1 expression. Therefore, in this report, we sort to determine whether inhibition of DCLK1 activity in the cisplatin resistant NSCLC could reverse cisplatin resistance and inhibiting tumor stem cell like phenotype.

DCLK1 has been shown to regulate key properties that enhance tumorigenesis.[17,18,21,22,40] Thus, we predicted that DCLK1 would have similar results in NSCLC. In accordance with the previous reports on the tumorigenic role of DCLK1 in colon, pancreas, kidney, and liver tumors, we observed reduced NSCLC cell proliferation, colony formation, migration, invasion, and self-renewal *in vitro* following DCLK1 knockdown.[18–20,22,24,41,42] Furthermore, DCLK1 silencing demonstrated tumor xenograft growth arrest and tumor regression *in vivo*. The ability of primary spheroid to form secondary spheroids is an essential feature of TSCs.[43,44] Interestingly, in our study, we found that the generation of secondary spheroid from primary spheroids in NSCLC cells was completely blocked following DCLK1 knockdown. Secondary spheroid growth can also be used as a surrogate for clonogenicity associated with TSCs. This is supported by our findings that DCLK1 knockdown not only prevented secondary spheroid formation but also reduced several stem cell proteins and pluripotency factors.

The acquisition of cisplatin resistance is the major cause of the mortality associated with patients with NSCLC.[45,46] We hypothesize that the acquisition of cisplatin resistance occurs via a DCLK1-mediated mechanism that involves the development of stem cell-like features with a particular emphasis on self-renewal. It is recently reported that miR539 is critical in reversing the resistance of NSCLC cells to cisplatin; however, the same study observed that restoration of DCLK1 overcame *miR539* and enhanced cisplatin resistance, although the study's main focus was on miR539.[47] Here we demonstrate that DCLK1 expression is the key factor in regulating the gain of resistance to cisplatin. Cisplatin resistance NSCLC cells have 3- to 4-fold increased self-renewal capacity and a 9-fold increase in the IC_{50} value compared with cisplatin-sensitive cells. Addition of siRNA against *DCLK1* in cisplatin resistance cells to low-dose cisplatin (5 μM, which is an 11-fold reduced dose than the original IC_{50} concentration of 57.42 μM) resulted in more than 90% cell death compared with cisplatin alone treatment. Furthermore, a similar combination of treatment completely abrogated the self-renewal

the number of spheroids between A549 and A549-CR cells. (E) DCLK1 expression increased with a gain of cisplatin resistance. *DCLK1* mRNA expression by RT-PCR and protein expression by western blot analysis. (F) Bar graph represents % cell viability between various treatment groups. (G) A549-CR cells treated with cisplatin at 40 μM or siDCLK1 transfection alone reduced the self-renewal ability of therapy-resistant tumor cells compared with vehicle treatment. A549-CR cells treated with cisplatin 5 μM 24 h after siDCLKL1 transfection almost completely abrogated tumor cell self-renewal ability compared with the individual treatments. (H) Bar graph represents the number of spheroids between various treatment groups. (G and H) Asterisks (*) indicate compared with control; number signs (#) represent compared with cisplatin (40 μM); dollar signs ($) indicate compared with siDCLK1. All quantitative data are expressed as mean ± SD of a minimum of five independent experiments. *$p < 0.05$, **$p < 0.01$, and ***$p < 0.001$ were considered statistically significant.

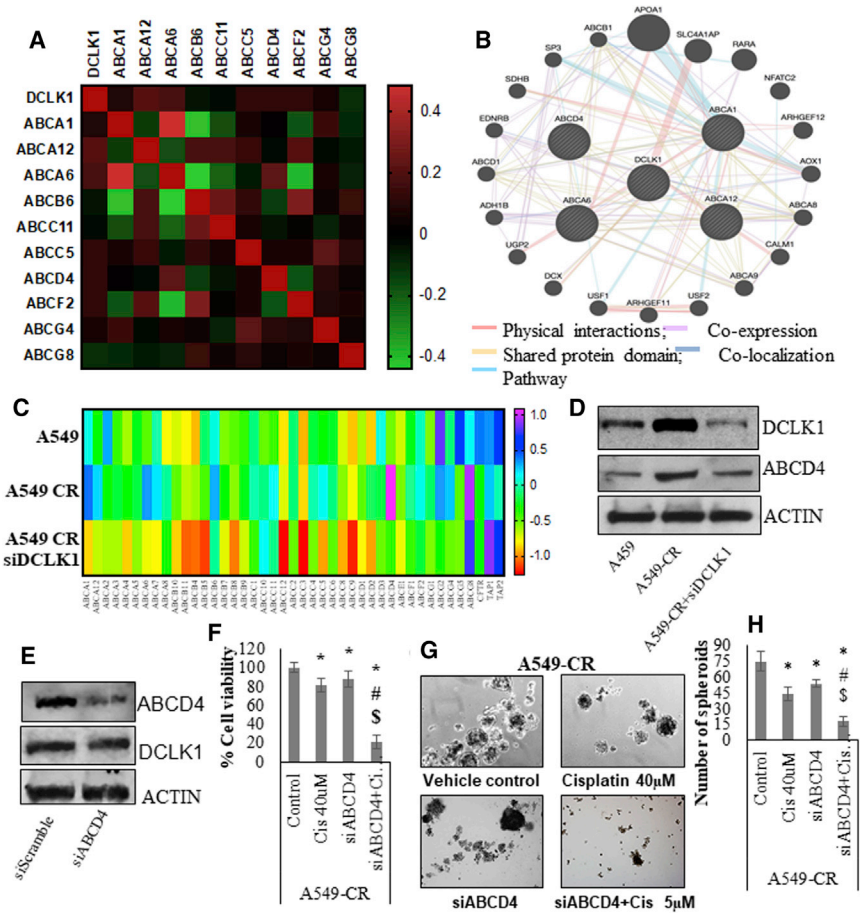

Figure 6. DCLK1-Associated Resistance to Cisplatin Is via an ABCD4-Mediated Mechanism

(A) *DCLK1* mRNA and mRNA of ABC transporters (*ABCA1, ABCA12, ACBA6, ABCB6, ABCC11, ABCC5, ABCD4, ABCF2, ABCG4, ABCG8*) were downloaded from the LUAD dataset of TCGA database. *DCLK1* expression is positively correlated with genes of ABC transporters; color indicates a correlation of *DCLK1* and other genes, negative (green) and positive (red). (B) Gene network from GeneMANIA shows the relationships for genes from the list (nodes) connected (with edges) according to the functional association networks from the databases. Based on the physical interactions, pathway, and genetic interactions, in the network representation, all of the nodes are connected and related to *DCLK1*. (C) cDNA from the A549 parental cells, A549-CR cells, and A549-CR cells treated with siDCLK1 were used to run the TaqMan human ABC transporters arrays. Heatmap depicting the upregulation of ABC transporters in the A549-CR cells compared with A549 cells, and siDCLK1 treatment reversed ABC upregulation. (D) Western blot for protein expression analysis for DCLK1 and ABCD4 between A549 cells, A549-CR cells, and A549-CR cells treated with siDCLK1. (E) Western blot representing the protein expression of DCLK1 and ABCD4 in A549-CR after scramble or siDCLK1 treatment. (F) Bar graph represents % cell viability between various treatment groups. (G) A549-CR treated with cisplatin at 40 μM or siABCD4 transfection alone moderately reduced the self-renewal ability of therapy-resistant tumor cells compared with vehicle treatment. A549-CR cells treated with cisplatin 5 μM 24 h after siABCD4 transfection significantly reduced the tumor cell self-renewal ability compared with the individual treatments. (H) Bar graph represents the number of spheroids between various treatment groups. (F and H) Asterisks (*) indicate compared with control; number signs (#) represent compared with cisplatin (40 μM); dollar signs ($) indicate compared with siABCD4. All quantitative data are expressed as mean ± SD of a minimum of five independent experiments. p values <0.05 are considered statistically significant.

capacity to cisplatin resistance NSCLC cells. In accordance with the present study, recent reports have demonstrated that the inhibition of protein kinases AKT/PI3K and STAT3 reduced cancer stemness and reversed cisplatin resistance in NSCLC.[48,49] Taken together, the present data strongly suggest that combining DCLK1 knockdown with cisplatin therapy may overcome the acquisition of resistance associated with cisplatin treatment.

Our study provides a complete overview of DCLK1-mediated NSCLC cisplatin resistance and associated enhanced self-renewal; however, the mechanism by which DCLK1 induces NSCLC cisplatin resistance is completely unknown. Several recent reports have implicated that ABC transporters play a critical role in the development of resistance to cisplatin in lung cancer.[11,12] Here we demonstrate that ABCD4 is the only ABC transporter that is highly expressed in cisplatin resistance NSCLC cells and is completely dependent on DCLK1 expression. Further, our data also provide the evidence that ABCD4 is the downstream target of DCLK1. Similarly, the combination of siABCD4 + low-dose cisplatin also demonstrated the loss of cell viability and abrogation of the self-renewal ability of cisplatin resistance NSCLC cells. Taken together, our study demonstrated that DCLK1 is critical in the gain of cisplatin resistance and associated enhanced self-renewal potency, which is critical for tumor progression, metastasis, and possibly tumor recurrence.[40,42,50]

Conclusions

Our findings demonstrate the acquisition of stem-like features following cisplatin treatment in NSCLC. These studies identified a novel therapeutic target for the effective treatment of cisplatin resistance NSCLC, which has been essentially undruggable. Furthermore, in this report, we suggest that cisplatin resistance may be related to resistance seen in other chemotherapeutic agents due to a common acquisition of stem cell-like features. Finally, we have provided evidence that targeting DCLK1 in NSCLC either alone or in combination

with cisplatin may be an effective strategy to combat NSCLC, most importantly the platinum-resistant NSCLCs.

MATERIALS AND METHODS

Pathological Characterization of Human Lung Cancer Tissue

Human lung cancer tissue microarrays (US Biomax HLug-Ade150-Sur-02) containing LUAD tissue from 75 cases and matched normal adjacent tissue (1 core/case) were stained with DCLK1 antibody (ab31704) following a previously described IHC protocol.[17,51] Each stained tissue micro-section was scored independently by two pathologists and based on the percent of tissue demonstrating staining (1 for <10% to 4 for >60%) and staining intensity (1 for lowest intensity and 4 for highest intensity). The resulting scores were multiplied by each other to obtain a composite score.

Analysis of TCGA LUAD Patient Data

The standard data run from TCGA's LUAD dataset from 706 patients was downloaded from the University of California, Santa Cruz (UCSC) cancer genome browser (http://xena.ucsc.edu/welcome-to-ucsc-xena/). Data were sorted and analyzed using the R statistical environment (version 3.0.2) as previously described.[20,22]

Determination of DCLK1-Correlated Stem Cell Factors, EMT Factors, and ABC Transporters in LUAD Patient Data

The LUAD RNA-seq datasets in TCGA dataset were downloaded through the UCSC cancer genome browser, as previously described.[22,40] Samples with high/low *DCLK1* expression levels were sorted by R v.3.2. Patients whose *DCLK1* expression levels were in the top 25% or bottom 25% were considered *DCLK1*-high or *DCLK1*-low, respectively. The corrplot function (R package corrplot) was used to confirm the correlation between the expression levels of *DCLK1* and other genes.

DCLK1 Network with Stem Cell Factors Utilizing the GeneMANIA Database

Datasets, including physical interactions, co-expression, pathway, and genetic interactions, were collected from the public domain GeneMANIA database. The dataset relevant to *DCLK1* and the stem cell factors network was generated from the GeneMANIA database (http://genemania.org).

Cell Culture

A549, H460, and H1299 human NSCLC cell lines and MRC9 human non-malignant lung cell line were obtained from ATCC and grown in Dulbecco's modified Eagle's medium with 4.5 g/L glucose and L-glutamine (Cellgro) supplemented with 10% fetal bovine serum (Sigma) at 37°C and 5% CO_2.

siRNA-Mediated Knockdown of *DCLK1* or *ABCD4*

Human NSCLC cells were seeded into 6-cm Petri dishes and allowed to attach overnight. Following attachment, 1 nM commercially validated siRNA against *DCLK1* (siDCLK1) or *ABCD4* (siABCD4) (Santa Cruz Biotech, USA) or 1 nM human scrambled sequence (siSCR) not targeting any known genes (Santa Cruz Biotech, USA) was complexed with Lipofectamine 3000 (Invitrogen) and added to the dishes in fresh cell culture minimum essential medium (MEM) medium. After 48 h, cells were used for further analysis.

Clonogenic Assay

NSCLC cells were plated in 48-well ultra-low-attachment plates at a density of 1,000 cells/well in RPMI medium containing 50% growth factor reduced Matrigel. The Matrigel cell suspensions were maintained and monitored for spheroid formation, as described previously.[17,18,22,27,51] For the secondary spheroid formation, primary spheroids were first recovered after the addition of corning cell recovery solution (Catalog No. 354253; Corning), which depolymerizes the Matrigel matrix and can be used to recover the spheroids. To dissociate the primary spheroids for single-cell suspensions, we incubated the primary spheroids with TrypLE for 20 min at 37°C. Single cells collected from the primary spheroids were plated for secondary spheroids formation as similar to primary spheroid generation.

Live/Dead Assays

NSCLC cells were seeded into a 96-well plate at 10^4 cells/well and allowed to attach overnight at 37°C. Post-treatment, fluorescent Live/Dead cell viability (Thermo Fisher Scientific, USA) assay was performed according to the manufacturer's protocol.

Generation of Cisplatin Resistance in NSCLC Cells

CR variant of A549 cell line as derived from its original parental cell line by continuous exposure to cisplatin (Sigma-Aldrich, USA) following initial dose-response studies of cisplatin over 72 h from which IC_{50} values were obtained. Initially, the CR subline was treated with cisplatin (IC_{50}) for 72 h. The media were removed, and cells were allowed to recover for a further 72 h. This development period was carried out for approximately 3 months, after which time IC_{50} concentrations were re-assessed in each resistant cell line. Cells were then maintained continuously in the presence of cisplatin at these new IC_{25} concentrations for a further 3 months.

TaqMan Array Human ABC Transporters in NSCLC Cells

The TaqMan array human ABC transporter (Cat. No. 4414166; Thermo Fisher Scientific, USA) contains 44 human ABC transporter genes and 4 proposed reference genes. We utilize gene-specific probe and primer sets to compare gene expression between A549 cells, A549-CR cells, and A549-CR cells treated with siDCLK1. The arrays were carried out according to the manufacturer's instructions. In brief, 10 μL cDNA was used as a template for the measurement of mRNA in quantitative PCR (qPCR). RT-PCR was performed using TaqMan Universal Master Mix from Thermo Fisher Scientific, USA. Thermal cycling conditions were as follows: 95°C for 10 min, then 95°C for 20 s and 60°C for 30 s for 40 cycles. Raw Cq values with automatically selected thresholds were calculated. The expression level of each gene for all samples was analyzed in triplicate and required at least two valid wells.

Cell Proliferation Assays

Cells (10^4 cells/well) were seeded into a 96-well tissue culture plate in triplicate. Post-treatment, 10 μL TACS MTT Reagent (RND Systems) was added to each well, and the cells were incubated at 37°C until a dark crystalline precipitate became visible in the cells. Then 100 μL of 266 mM NH_4OH in DMSO was added to the wells and placed on a plate shaker at low speed for 5 min. After shaking, the plate was allowed to incubate for 10 min protected from light, and the OD_{550} for each well was read using a microplate reader. The results were averaged and calculated as percentage cell proliferation.

Migration and Invasion Assay

For the invasion assay, Matrigel-coated Transwells (BD Biosciences) were prepared by retrieving in serum-free media for 2 h at 37°C. For the migration assay, Transwells (BD Biosciences) were used. Subsequently, cells (5,000/well) pre-transfected with either 1 nM siRNA or siSCR for 48 h were seeded into each Transwell in triplicate in serum-free media, or cells post-treated with cisplatin were used. Cell culture medium containing 10% FBS was added to the bottom of each well as a chemoattractant, and the cells were incubated for 24 h at 37°C under 5% CO_2. Afterward, a cotton swab was used to scrape non-invasive or non-migratory cells off the top of Transwells; the remaining cells were fixed and stained with 0.1% crystal violet and allowed to dry. After drying, all invading or migrating cells were counted from each Transwell. Results are reported as the percentage of cells invaded and/or migrated.

Colony Formation Assay

NSCLC cells were transiently transfected with si-DCLK1 or scramble siRNA or post-treated with cisplatin or combinatorial treatments. After 48 h, cells were seeded and passaged into new six-well plates (100 cells/well). Cells were allowed to grow for 1 week, fixed with glacial acetic acid/methanol solution (1:3), and washed with PBS. Colonies were stained with 0.1% crystal violet for 10 min and were washed with tap water to remove excess stain. Colonies were then counted under a stereomicroscope using a 1-cm^2 grid. Four squares from four quadrants were counted for each well.

Quantitative Real-Time RT-PCR

Total RNA was isolated from NSCLC cells using Tri Reagent (MRC) per the manufacturer's instructions. First-strand cDNA synthesis was carried out using SuperScript II Reverse Transcriptase and random hexanucleotide primers (Invitrogen). The complementary DNA was subsequently used to perform RT-PCR on an iCycler IQ5 Thermal Cycler (Bio-Rad) using SYBR Green (Molecular Probes) with gene-specific primers and JumpStart Taq DNA polymerase (Sigma). The crossing threshold value assessed was normalized to β-actin, and quantitative changes in mRNA were expressed as fold-change relative to control ± SD value.

Immunoblot Analysis

Twenty-five micrograms of the total protein was size separated in a 4%–12% SDS polyacrylamide gel and transferred electrophoretically onto a polyvinylidene fluoride (PVDF) membrane with a wet-blot transfer apparatus (Bio-Rad, Hercules, CA, USA). The membrane was blocked and incubated overnight with a primary antibody, and was subsequently incubated with a horseradish peroxidase-conjugated secondary antibody. The proteins were detected using enhanced chemiluminescence (ECL) western blotting detection reagents (Amersham-Pharmacia, Piscataway, NJ, USA). Protein density quantification was performed with GelQuant software. Actin (42-kDa) was used as a loading control.

IHC/Immunofluorescence

Standard IHC protocols were used with specific antibodies, as described previously.[51–53]

IHC

Heat-induced epitope retrieval was performed on 4-μm formalin-fixed, paraffin-embedded sections utilizing a pressurized Decloaking Chamber (Biocare Medical, Concord, CA, USA) in citrate buffer (pH 6.0) at 99°C for 18 min.

Bright Field

Slides were incubated in 3% hydrogen peroxide at room temperature for 10 min. After incubation with the primary antibody overnight at 4°C, slides were incubated in a Promark peroxidase-conjugated polymer detection system (Biocare Medical) for 30 min at room temperature. After washing, slides were devolved with diaminobenzidine (Sigma-Aldrich).

Image Acquisition

Slides were examined on the Nikon Eclipse Ti motorized microscope paired with image app operated by the NIS-Elements Microscope Imaging Software platform (Nikon Instruments, Melville, NY, USA).

Cisplatin Concentration Assay

After cisplatin treatment, cells were washed twice with PBS, and cell lysate was prepared using cell lysis buffer. After a 10-min centrifugation at 15,000 rpm at 4°C, the supernatant was used to determine protein concentration. The cisplatin concentrations in the supernatant were measured by a cisplatin assay kit (MicroMolar Cisplatin Assay Kit; ProFoldin). The samples, buffer, and chelate color solution were mixed and incubated for 60 min at 65°C. The absorbance was then read at a wavelength of 535 nm using a microplate reader. The platinum reading was normalized to protein concentration.

Animals

All animal experiments were performed with approval and authorization from the Institutional Review Board and the Institutional Animal Care and Use Committee at the University of Oklahoma Health Sciences Center (Oklahoma City, OK, USA). Athymic nude mice were obtained from The Jackson Laboratory and were maintained.

Synthesis and Characterization of *DCLK1* siRNA NPs and Treatment

PLGA NPs were synthesized using a double-emulsion solvent evaporation technique as described previously.[18] The amount of

encapsulated siRNA was quantified using a spectrophotometer (DU-800; Beckman Coulter, Brea, CA, USA). The size, polydispersity index, and zeta-potential measurements of synthesized siRNA NPs were determined using diffraction light scattering (DLS) and utilizing Zeta PALS (Brookhaven Instruments, Holtsville, NY, USA). Tumor xenograft athymic nude mice were injected i.p. with 0.25 nmol siRNA preparation on every third day for a total of six doses.

Xenograft Tumor Study

H460 cells (5×10^5) were injected subcutaneously into the flanks of athymic nude mice and allowed to grow until the tumor reached an average volume of 100 mm^3. Xenografts were injected i.p. with 0.25 nmol siRNA preparation on every third day for a total of six doses. Horizontal and vertical tumor diameters were measured on each injection date with calipers, and tumor volume was calculated using the following formula: tumor volume = 0.5 × length × $width^2$.

Statistical Analyses

All statistical analyses were performed in GraphPad Prism 6.0, SPSS Statistics 22, and Microsoft Excel. One-way ANOVA and the Student's t test were used to determine statistical significance. Pearson product-moment correlation was used for analysis and correlation of gene expressions between two groups. For survival analyses, the log rank (Mantel-Cox) test and the Gehan-Breslow-Wilcoxon test were used. *$p < 0.05$, **$p < 0.01$, and ***$p < 0.001$ were considered statistically significant.

Ethics

All animal experiments were performed with the approval and authorization of the Institutional Review Board and the Institutional Animal Care and Use Committee, University of Oklahoma Health Sciences Center.

Data Availability

The datasets analyzed during the current study are available from the corresponding author upon reasonable request.

SUPPLEMENTAL INFORMATION

Supplemental Information can be found online at https://doi.org/10.1016/j.omto.2020.05.012.

AUTHOR CONTRIBUTIONS

P.C. is the corresponding author and was responsible for conception and design, collection and/or assembly of data, data analysis and interpretation, and manuscript writing; J.P. conducted acquisition, assembly, and interpretation of data; P.M. generated bioinformatics data; R.P., H.G., M.L., K.K., and D.N. generated CR cell lines and analyzed data; N.W. and D.Q. analyzed and interpreted data; K.P. analyzed data; S.L. is a pathologist and was responsible for pathological evaluation and scoring; C.R. provided material support, collection, and interpretation of data; M.B. provided material support, and analyzed and interpreted data; and C.H. assisted in writing the manuscript. All authors discussed the results, analyzed data, and edited the manuscript. All authors are aware of the content and agree with the submission.

CONFLICTS OF INTEREST

C.H. is the co-founder of COARE Holdings, USA. The other authors declare no competing interests.

ACKNOWLEDGMENTS

This work was supported by the Department of Defense, USA, grant ID: W81XWH-18-1-0457 (PI, Parthasarathy Chandrakesan). We thank the Stephenson Cancer Center CORE facility at OUHSC for histological services.

REFERENCES

1. Siegel, R., Ma, J., Zou, Z., and Jemal, A. (2014). Cancer statistics, 2014. CA Cancer J. Clin. *64*, 9–29.
2. Torre, L.A., Siegel, R.L., and Jemal, A. (2016). Lung Cancer Statistics. Adv. Exp. Med. Biol. *893*, 1–19.
3. Denisenko, T.V., Budkevich, I.N., and Zhivotovsky, B. (2018). Cell death-based treatment of lung adenocarcinoma. Cell Death Dis. *9*, 117.
4. Mitsudomi, T., Morita, S., Yatabe, Y., Negoro, S., Okamoto, I., Tsurutani, J., Seto, T., Satouchi, M., Tada, H., Hirashima, T., et al.; West Japan Oncology Group (2010). Gefitinib versus cisplatin plus docetaxel in patients with non-small-cell lung cancer harbouring mutations of the epidermal growth factor receptor (WJTOG3405): an open label, randomised phase 3 trial. Lancet Oncol. *11*, 121–128.
5. Dean, M., Fojo, T., and Bates, S. (2005). Tumour stem cells and drug resistance. Nat. Rev. Cancer *5*, 275–284.
6. Jeter, C.R., Liu, B., Liu, X., Chen, X., Liu, C., Calhoun-Davis, T., Repass, J., Zaehres, H., Shen, J.J., and Tang, D.G. (2011). NANOG promotes cancer stem cell characteristics and prostate cancer resistance to androgen deprivation. Oncogene *30*, 3833–3845.
7. Sławek, S., Szmyt, K., Fularz, M., Dziudzia, J., Boruczkowski, M., Sikora, J., and Kaczmarek, M. (2016). Pluripotency transcription factors in lung cancer-a review. Tumour Biol. *37*, 4241–4249.
8. Zhou, B.B., Zhang, H., Damelin, M., Geles, K.G., Grindley, J.C., and Dirks, P.B. (2009). Tumour-initiating cells: challenges and opportunities for anticancer drug discovery. Nat. Rev. Drug Discov. *8*, 806–823.
9. Sosa Iglesias, V., Giuranno, L., Dubois, L.J., Theys, J., and Vooijs, M. (2018). Drug Resistance in Non-Small Cell Lung Cancer: A Potential for NOTCH Targeting? Front. Oncol. *8*, 267.
10. Shibue, T., and Weinberg, R.A. (2017). EMT, CSCs, and drug resistance: the mechanistic link and clinical implications. Nat. Rev. Clin. Oncol. *14*, 611–629.
11. Su, J., Wu, S., Tang, W., Qian, H., Zhou, H., and Guo, T. (2016). Reduced SLC27A2 induces cisplatin resistance in lung cancer stem cells by negatively regulating Bmi1-ABCG2 signaling. Mol. Carcinog. *55*, 1822–1832.
12. Subhani, S., Jayaraman, A., and Jamil, K. (2015). Homology modelling and molecular docking of MDR1 with chemotherapeutic agents in non-small cell lung cancer. Biomed. Pharmacother. *71*, 37–45.
13. Galluzzi, L., Vitale, I., Michels, J., Brenner, C., Szabadkai, G., Harel-Bellan, A., Castedo, M., and Kroemer, G. (2014). Systems biology of cisplatin resistance: past, present and future. Cell Death Dis. *5*, e1257.
14. Salem, A., Asselin, M.C., Reymen, B., Jackson, A., Lambin, P., West, C.M.L., O'Connor, J.P.B., and Faivre-Finn, C. (2018). Targeting Hypoxia to Improve Non-Small Cell Lung Cancer Outcome. J. Natl. Cancer Inst. *110*, 14–30.
15. Bailey, J.M., Alsina, J., Rasheed, Z.A., McAllister, F.M., Fu, Y.Y., Plentz, R., Zhang, H., Pasricha, P.J., Bardeesy, N., Matsui, W., et al. (2014). DCLK1 marks a morphologically distinct subpopulation of cells with stem cell properties in preinvasive pancreatic cancer. Gastroenterology *146*, 245–256.
16. Nakanishi, Y., Seno, H., Fukuoka, A., Ueo, T., Yamaga, Y., Maruno, T., Nakanishi, N., Kanda, K., Komekado, H., Kawada, M., et al. (2013). Dclk1 distinguishes between tumor and normal stem cells in the intestine. Nat. Genet. *45*, 98–103.

17. Chandrakesan, P., Roy, B., Jakkula, L.U., Ahmed, I., Ramamoorthy, P., Tawfik, O., Papineni, R., Houchen, C., Anant, S., and Umar, S. (2014). Utility of a bacterial infection model to study epithelial-mesenchymal transition, mesenchymal-epithelial transition or tumorigenesis. Oncogene *33*, 2639–2654.

18. Chandrakesan, P., Weygant, N., May, R., Qu, D., Chinthalapally, H.R., Sureban, S.M., Ali, N., Lightfoot, S.A., Umar, S., and Houchen, C.W. (2014). DCLK1 facilitates intestinal tumor growth via enhancing pluripotency and epithelial mesenchymal transition. Oncotarget *5*, 9269–9280.

19. Weygant, N., Qu, D., May, R., Tierney, R.M., Berry, W.L., Zhao, L., Agarwal, S., Chandrakesan, P., Chinthalapally, H.R., Murphy, N.T., et al. (2015). DCLK1 is a broadly dysregulated target against epithelial-mesenchymal transition, focal adhesion, and stemness in clear cell renal carcinoma. Oncotarget *6*, 2193–2205.

20. Weygant, N., Ge, Y., Qu, D., Kaddis, J.S., Berry, W.L., May, R., Chandrakesan, P., Bannerman-Menson, E., Vega, K.J., Tomasek, J.J., et al. (2016). Survival of Patients with Gastrointestinal Cancers Can Be Predicted by a Surrogate microRNA Signature for Cancer Stem-like Cells Marked by DCLK1 Kinase. Cancer Res. *76*, 4090–4099.

21. Nguyen, C.B., Kotturi, H., Waris, G., Mohammed, A., Chandrakesan, P., May, R., Sureban, S., Weygant, N., Qu, D., Rao, C.V., et al. (2016). (Z)-3,5,4′-Trimethoxystilbene Limits Hepatitis C and Cancer Pathophysiology by Blocking Microtubule Dynamics and Cell-Cycle Progression. Cancer Res. *76*, 4887–4896.

22. Chandrakesan, P., Yao, J., Qu, D., May, R., Weygant, N., Ge, Y., Ali, N., Sureban, S.M., Gude, M., Vega, K., et al. (2017). Dclk1, a tumor stem cell marker, regulates pro-survival signaling and self-renewal of intestinal tumor cells. Mol. Cancer *16*, 30.

23. Omori, Y., Suzuki, M., Ozaki, K., Harada, Y., Nakamura, Y., Takahashi, E., and Fujiwara, T. (1998). Expression and chromosomal localization of KIAA0369, a putative kinase structurally related to Doublecortin. J. Hum. Genet. *43*, 169–177.

24. Weygant, N., Qu, D., Berry, W.L., May, R., Chandrakesan, P., Owen, D.B., Sureban, S.M., Ali, N., Janknecht, R., and Houchen, C.W. (2014). Small molecule kinase inhibitor LRRK2-IN-1 demonstrates potent activity against colorectal and pancreatic cancer through inhibition of doublecortin-like kinase 1. Mol. Cancer *13*, 103.

25. Ito, K., and Suda, T. (2014). Metabolic requirements for the maintenance of self-renewing stem cells. Nat. Rev. Mol. Cell Biol. *15*, 243–256.

26. Wang, S., Gao, D., and Chen, Y. (2017). The potential of organoids in urological cancer research. Nat. Rev. Urol. *14*, 401–414.

27. Chandrakesan, P., May, R., Qu, D., Weygant, N., Taylor, V.E., Li, J.D., Ali, N., Sureban, S.M., Qante, M., Wang, T.C., et al. (2015). Dclk1+ small intestinal epithelial tuft cells display the hallmarks of quiescence and self-renewal. Oncotarget *6*, 30876–30886.

28. Calvet, C.Y., André, F.M., and Mir, L.M. (2014). The culture of cancer cell lines as tumorspheres does not systematically result in cancer stem cell enrichment. PLoS ONE *9*, e89644.

29. Felthaus, O., Ettl, T., Gosau, M., Driemel, O., Brockhoff, G., Reck, A., Zeitler, K., Hautmann, M., Reichert, T.E., Schmalz, G., and Morsczeck, C. (2011). Cancer stem cell-like cells from a single cell of oral squamous carcinoma cell lines. Biochem. Biophys. Res. Commun. *407*, 28–33.

30. Herbst, R.S., Morgensztern, D., and Boshoff, C. (2018). The biology and management of non-small cell lung cancer. Nature *553*, 446–454.

31. Baek, N., Seo, O.W., Lee, J., Hulme, J., and An, S.S. (2016). Real-time monitoring of cisplatin cytotoxicity on three-dimensional spheroid tumor cells. Drug Des. Devel. Ther. *10*, 2155–2165.

32. Lhuissier, E., Bazille, C., Aury-Landas, J., Girard, N., Pontin, J., Boittin, M., Boumediene, K., and Baugé, C. (2017). Identification of an easy to use 3D culture model to investigate invasion and anticancer drug response in chondrosarcomas. BMC Cancer *17*, 490.

33. Drost, J., and Clevers, H. (2018). Organoids in cancer research. Nat. Rev. Cancer *18*, 407–418.

34. Liu, J.J., Lu, J., and McKeage, M.J. (2012). Membrane transporters as determinants of the pharmacology of platinum anticancer drugs. Curr. Cancer Drug Targets *12*, 962–986.

35. Domenichini, A., Adamska, A., and Falasca, M. (2019). ABC transporters as cancer drivers: Potential functions in cancer development. Biochim. Biophys. Acta, Gen. Subj. *1863*, 52–60.

36. Robey, R.W., Pluchino, K.M., Hall, M.D., Fojo, A.T., Bates, S.E., and Gottesman, M.M. (2018). Revisiting the role of ABC transporters in multidrug-resistant cancer. Nat. Rev. Cancer *18*, 452–464.

37. Chen, Z., Fillmore, C.M., Hammerman, P.S., Kim, C.F., and Wong, K.K. (2014). Non-small-cell lung cancers: a heterogeneous set of diseases. Nat. Rev. Cancer *14*, 535–546.

38. Rotow, J., and Bivona, T.G. (2017). Understanding and targeting resistance mechanisms in NSCLC. Nat. Rev. Cancer *17*, 637–658.

39. Chen, X., Xie, W., Gu, P., Cai, Q., Wang, B., Xie, Y., Dong, W., He, W., Zhong, G., Lin, T., and Huang, J. (2015). Upregulated WDR5 promotes proliferation, self-renewal and chemoresistance in bladder cancer via mediating H3K4 trimethylation. Sci. Rep. *5*, 8293.

40. Ge, Y., Weygant, N., Qu, D., May, R., Berry, W.L., Yao, J., Chandrakesan, P., Zheng, W., Zhao, L., Zhao, K.L., et al. (2018). Alternative splice variants of DCLK1 mark cancer stem cells, promote self-renewal and drug-resistance, and can be targeted to inhibit tumorigenesis in kidney cancer. Int. J. Cancer *143*, 1162–1175.

41. Ali, N., Allam, H., May, R., Sureban, S.M., Bronze, M.S., Bader, T., Umar, S., Anant, S., and Houchen, C.W. (2011). Hepatitis C virus-induced cancer stem cell-like signatures in cell culture and murine tumor xenografts. J. Virol. *85*, 12292–12303.

42. Chandrakesan, P., Panneerselvam, J., Qu, D., Weygant, N., May, R., Bronze, M.S., and Houchen, C.W. (2016). Regulatory Roles of Dclk1 in Epithelial Mesenchymal Transition and Cancer Stem Cells. J. Carcinog. Mutagen. *7*, 257.

43. Lee, C.H., Yu, C.C., Wang, B.Y., and Chang, W.W. (2016). Tumorsphere as an effective in vitro platform for screening anti-cancer stem cell drugs. Oncotarget *7*, 1215–1226.

44. Cao, L., Zhou, Y., Zhai, B., Liao, J., Xu, W., Zhang, R., Li, J., Zhang, Y., Chen, L., Qian, H., et al. (2011). Sphere-forming cell subpopulations with cancer stem cell properties in human hepatoma cell lines. BMC Gastroenterol. *11*, 71.

45. Morgillo, F., Della Corte, C.M., Fasano, M., and Ciardiello, F. (2016). Mechanisms of resistance to EGFR-targeted drugs: lung cancer. ESMO Open *1*, e000060.

46. Chan, B.A., and Hughes, B.G. (2015). Targeted therapy for non-small cell lung cancer: current standards and the promise of the future. Transl. Lung Cancer Res. *4*, 36–54.

47. Deng, H., Qianqian, G., Ting, J., and Aimin, Y. (2018). miR-539 enhances chemosensitivity to cisplatin in non-small cell lung cancer by targeting DCLK1. Biomed. Pharmacother. *106*, 1072–1081.

48. Zhang, Y., Bao, C., Mu, Q., Chen, J., Wang, J., Mi, Y., Sayari, A.J., Chen, Y., and Guo, M. (2016). Reversal of cisplatin resistance by inhibiting PI3K/Akt signal pathway in human lung cancer cells. Neoplasma *63*, 362–370.

49. MacDonagh, L., Gray, S.G., Breen, E., Cuffe, S., Finn, S.P., O'Byrne, K.J., and Barr, M.P. (2018). BBI608 inhibits cancer stemness and reverses cisplatin resistance in NSCLC. Cancer Lett. *428*, 117–126.

50. Pisco, A.O., and Huang, S. (2015). Non-genetic cancer cell plasticity and therapy-induced stemness in tumour relapse: 'What does not kill me strengthens me'. Br. J. Cancer *112*, 1725–1732.

51. Chandrakesan, P., May, R., Weygant, N., Qu, D., Berry, W.L., Sureban, S.M., Ali, N., Rao, C., Huycke, M., Bronze, M.S., and Houchen, C.W. (2016). Intestinal tuft cells regulate the ATM mediated DNA Damage response via Dclk1 dependent mechanism for crypt restitution following radiation injury. Sci. Rep. *6*, 37667.

52. Chandrakesan, P., Ahmed, I., Anwar, T., Wang, Y., Sarkar, S., Singh, P., Peleg, S., and Umar, S. (2010). Novel changes in NF-kappaB activity during progression and regression phases of hyperplasia: role of MEK, ERK, and p38. J. Biol. Chem. *285*, 33485–33498.

53. Chandrakesan, P., Ahmed, I., Chinthalapally, A., Singh, P., Awasthi, S., Anant, S., and Umar, S. (2012). Distinct compartmentalization of NF-κB activity in crypt and crypt-denuded lamina propria precedes and accompanies hyperplasia and/or colitis following bacterial infection. Infect. Immun. *80*, 753–767.